PLOS Computational Biology

Neural coding in the visual system of Drosophila melanogaster: How do small neural populations support visually guided behaviours?

--Manuscript Draft--

Manuscript Number:	PCOMPBIOL-D-17-00746
Full Title:	Neural coding in the visual system of Drosophila melanogaster: How do small neural populations support visually guided behaviours?
Short Title:	Neural coding of information for visual behaviours in Drosophila
Article Type:	Research Article
Keywords:	Drosophila melanogaster; ring neurons; ellipsoid body; central complex; neural coding; visual behaviour; computational neuroscience
Corresponding Author:	Alex David McDonald Dewar University of Sussex Falmer, East Sussex UNITED KINGDOM
Corresponding Author Secondary Information:	
Corresponding Author's Institution:	University of Sussex
Corresponding Author's Secondary Institution:	
First Author:	Alex David McDonald Dewar
First Author Secondary Information:	
Order of Authors:	Alex David McDonald Dewar
	Antoine Wystrach
	Andrew Philippides
	Paul Graham
Order of Authors Secondary Information:	
Abstract:	All organisms wishing to survive and reproduce must be able to respond adaptively to a complex, changing world. Yet the computational power available is constrained by biology and evolution, favouring mechanisms that are parsimonious yet robust. Here we investigate the information carried in small populations of visually responsive neurons in Drosophila melanogaster. These so-called 'ring neurons', projecting to the ellipsoid body of the central complex, are reported to be necessary for complex visual tasks such as pattern recognition and visual navigation. Recently the receptive fields of these neurons have been mapped, allowing us to investigate how well they can support such behaviours. For instance, in a simulation of classic pattern discrimination experiments, we show that the patterns of output from the ring neurons matches observed fly behaviour. However, performance of the neurons (as with flies) is not perfect and can be easily improved with the addition of extra neurons, suggesting the neurons' receptive fields are not optimised for recognising abstract shapes, a conclusion which casts doubt on cognitive explanations of fly behaviour in pattern recognition assays. Using artificial neural networks, we then assess how easy it is to decode more general information about stimulus shape from the ring neuron population codes. We show that these neurons are well-suited for encoding information about size, position and orientation, which are more relevant behavioural parameters for a fly than abstract pattern properties. This leads us to suggest that in order to understand the properties of neural systems, one must consider how perceptual circuits put information at the service of behaviour.
Suggested Reviewers:	Holk Cruse Universitat Bielefeld holk.cruse@uni-bielefeld.de

	Emily Baird Lunds Universitet emily.baird@biol.lu.se
	Andrew Barron Macquarie University andrew.barron@mq.edu.au
	Michael Mangan University of Lincoln mmangan@lincoln.ac.uk
Opposed Reviewers:	
Additional Information:	
Question	**Response**
Financial Disclosure Please describe all sources of funding that have supported your work. **This information is required for submission and will be published with your article, should it be accepted.** A complete funding statement should do the following: Include **grant numbers and the URLs** of any funder's website. Use the full name, not acronyms, of funding institutions, and use initials to identify authors who received the funding. **Describe the role** of any sponsors or funders in the study design, data collection and analysis, decision to publish, or preparation of the manuscript. If the funders had **no role** in any of the above, include this sentence at the end of your statement: "*The funders had no role in study design, data collection and analysis, decision to publish, or preparation of the manuscript.*" However, if the study was **unfunded**, please provide a statement that clearly indicates this, for example: "*The author(s) received no specific funding for this work.*" * typeset	AD, PG and AP are funded by EPSRC (grant code: EP/P006094/1; https://www.epsrc.ac.uk/). AW is funded by the Fyssen Foundation (http://www.fondationfyssen.fr/en/). AD and PG have also received funding from the BBSRC (grant codes: BB/F015925/1 and BB/H013644; http://www.bbsrc.ac.uk/). AP has also received funding from the European Union's Seventh Framework Programme for research, technological development and demonstration under grant agreement no. 308943 (https://ec.europa.eu/research/fp7/index_en.cfm).
Competing Interests You are responsible for recognizing and disclosing on behalf of all authors any competing interest that could be perceived to bias their work, acknowledging all financial support and any other relevant financial or non-financial competing interests.	The authors have declared that no competing interests exist.

Do any authors of this manuscript have competing interests (as described in the PLOS Policy on Declaration and Evaluation of Competing Interests)? **If yes**, please provide details about any and all competing interests in the box below. Your response should begin with this statement: *I have read the journal's policy and the authors of this manuscript have the following competing interests:* **If no** authors have any competing interests to declare, please enter this statement in the box: "*The authors have declared that no competing interests exist.*" * typeset	
Data Availability PLOS journals require authors to make all data underlying the findings described in their manuscript fully available, without restriction and from the time of publication, with only rare exceptions to address legal and ethical concerns (see the PLOS Data Policy and FAQ for further details). When submitting a manuscript, authors must provide a Data Availability Statement that describes where the data underlying their manuscript can be found. Your answers to the following constitute your statement about data availability and will be included with the article in the event of publication. **Please note that simply stating 'data available on request from the author' is not acceptable. *If, however, your data are only available upon request from the author(s), you must answer "No" to the first question below, and explain your exceptional situation in the text box provided.*** Do the authors confirm that all data underlying the findings described in their manuscript are fully available without restriction?	Yes - all data are fully available without restriction
Please describe where your data may be found, writing in full sentences. **Your answers should be entered into the box below and will be published in the form you provide them, if your manuscript is accepted.** If you are copying our sample text below, please ensure you replace any	Data will be made available in full (via figshare, according to the funders' and the University of Sussex's requirements) if the manuscript is accepted.

instances of XXX with the appropriate details. If your data are all contained within the paper and/or Supporting Information files, please state this in your answer below. For example, “All relevant data are within the paper and its Supporting Information files.” If your data are held or will be held in a public repository, include URLs, accession numbers or DOIs. For example, “All XXX files are available from the XXX database (accession number(s) XXX, XXX)." If this information will only be available after acceptance, please indicate this by ticking the box below. If neither of these applies but you are able to provide details of access elsewhere, with or without limitations, please do so in the box below. For example: “Data are available from the XXX Institutional Data Access / Ethics Committee for researchers who meet the criteria for access to confidential data.” “Data are from the XXX study whose authors may be contacted at XXX.” * typeset	
Additional data availability information:	Tick here if the URLs/accession numbers/DOIs will be available only after acceptance of the manuscript for publication so that we can ensure their inclusion before publication.

UNIVERSITY OF SUSSEX

Dear Sir/Madam,

We submit for your attention our manuscript, entitled: “Neural coding in the visual system of *Drosophila melanogaster*: How do small neural populations support visually guided behaviours?”, for inclusion in PLoS Computational Biology.

A general problem in neuroscience is understanding how sensory systems organise information to be at the service of behaviour. Computational approaches have always been important in this endeavour, as they allow one to simulate the sensory experience of a behaving animal whilst considering how this information is transformed by populations of neurons. Thus we can relate the details of neural circuitry to theories about the requirements of behaviour. In visual neuroscience, a rare opportunity has emerged to understand how visually guided behaviours are mediated by particular visual encodings. Specific small sub-populations of identifiable neurons in *Drosophila* are known to be necessary for particular visual tasks and the individual receptive fields of the neurons in these populations have now been described in detail. Surprisingly, these populations are small, with only twenty or so neurons, which suggests something of a sensory bottleneck. In our manuscript, we consider how the population code from these neurons relates to the information required to control specific behaviours in *Drosophila,* by analysing the neural outputs that result from simulations of classic *Drosophila* experiments. We conclude that, despite previous claims, *Drosophila* are unlikely to possess a general-purpose pattern-learning ability. However, information about the shape and size of objects necessary for some visually guided behaviours in *Drosophila* does pass through the sensory bottleneck. We feel that the general interest in visual coding, visually guided behaviour, biomimetics and in *Drosophila* neuroscience means that this paper is of general interest for your readership.

We take as our starting point the work of Seelig and Jayaraman (“Feature detection and orientation tuning in the Drosophila central complex.” *Nature*, 2013) who mapped the receptive fields properties of two groups of cells in the ellipsoid body of the central complex of *Drosophila*. Intriguingly, in contrast to mammalian simple cells, the receptive fields of these cells are very large (up to 90˚ in both elevation and azimuth) and the cell populations are very small in number (14 and 7 per eye for the two cell types). It is thought that sub-populations of these neurons serve pattern recognition and short-term memory for a bar’s location, respectively following classic behavioural experiments with flies. These abilities are lost when specific sub-populations of neurons are silenced. Our simulations reproduce fly performance and can even explain the surprisingly poor performance of *Drosophila* in discriminating some particular shape-pairs. However, crucially we show that pattern-learning performance can be improved easily through the addition of extra neurons, suggesting that this system might not be optimised through evolution for pattern recognition per se.

To consider more generally what information is preserved by these small networks of visually responsive neurons, we used artificial neural networks to ask how easy it is to decode more general information about stimulus shape from neural outputs. We show that these neurons are well-suited for encoding information about size, position and orientation, which are more relevant behavioural parameters for a fly than abstract pattern properties. Rather, the limited ability to discriminate patterns using abstract properties may well be a by-product arising from a simple visual system tuned to provide information to guide specific behaviours.

SCHOOL OF LIFE SCIENCES
University of Sussex | John Maynard Smith Building | Brighton BN2 9QG | United Kingdom
T +44 (0)1273 872943 | p.r.graham@sussex.ac.uk
www.sussex.ac.uk/lifesci/insectnavigation

This leads us to suggest that in order to understand the properties of neural systems, one must consider how perceptual circuits put information at the service of behaviour, rather than whether, or how, they preserve all of the detail in a visual scene. This work thus presents novel insights into the function of visual circuits in *Drosophila*, but also has broader implications for neural coding in other systems.

In recent times, PLoS Computational Biology has a track record of high impact publications in a range of topics in invertebrate visual neuroscience (e.g. Visual learning for navigation: Ardin et al. (2016) and Baddeley et al. (2012); Pattern recognition in bees: Roper and Chittka (2017)). Therefore, because of both the theme and the general interest of this work, we feel very strongly that PLoS Computational Biology is its ideal location. This manuscript has not been submitted to any other journal previously.

Yours Faithfully,

Dr Paul Graham
(On behalf of Dr Andrew Philippides, Dr Alex Dewar and Dr Antoine Wystrach)

Neural coding in the visual system of *Drosophila melanogaster*: How do small neural populations support visually guided behaviours?

Alex D. M. Dewar[1], Antoine Wystrach[2], Andrew Philippides[1], Paul Graham[3,*]

1 Alex D. M. Dewar and Andrew Philippides, Department of Informatics, Chichester I, University of Sussex, Falmer, BN1 9QJ, UK.

2 Antoine Wystrach, Centre de Recherches sur la Cognition Animale, Centre National de la Recherche Scientifique, Université Paul Sabatier, Toulouse, France.

3 Paul Graham, School of Life Sciences, John Maynard Smith Building, University of Sussex, Falmer, BN1 9QJ, UK.

∗ **E-mail: paulgr@sussex.ac.uk**

Abstract

All organisms wishing to survive and reproduce must be able to respond adaptively to a complex, changing world. Yet the computational power available is constrained by biology and evolution, favouring mechanisms that are parsimonious yet robust. Here we investigate the information carried in small populations of visually responsive neurons in *Drosophila melanogaster*. These so-called 'ring neurons', projecting to the ellipsoid body of the central complex, are reported to be necessary for complex visual tasks such as pattern recognition and visual navigation. Recently the receptive fields of these neurons have been mapped, allowing us to investigate how well they can support such behaviours. For instance, in a simulation of classic pattern discrimination experiments, we show that the patterns of output from the ring neurons matches observed fly behaviour. However, performance of the neurons (as with flies) is not perfect and can be easily improved with the addition of extra neurons, suggesting the neurons' receptive fields are not optimised for recognising abstract shapes, a conclusion which casts doubt on cognitive explanations of fly behaviour in pattern recognition assays. Using artificial neural networks, we then assess how easy it is to decode more general information about stimulus shape from the ring neuron population codes. We show that these neurons are well-suited for encoding information about size, position and orientation, which are more relevant behavioural parameters for a fly than abstract pattern properties. This leads us to suggest that in order to understand the properties of neural systems, one

must consider how perceptual circuits put information at the service of behaviour.

Author Summary

A general problem in neuroscience is understanding how sensory systems organise information to be at the service of behaviour. Computational approaches can be useful for such studies as they allow one to simulate the sensory experience of a behaving animal whilst considering how sensory information should be encoded. In flies, small subpopulations of identifiable neurons are known to be necessary for particular visual tasks, and the response properties of these populations have now been described in detail. Surprisingly, these populations are small, with only twenty or so neurons, which suggests something of a sensory bottleneck. In this paper, we consider how the population code from these neurons relates to the information required to control specific behaviours. We conclude that, despite previous claims, flies are unlikely to possess a general-purpose pattern-learning ability. However, implicit information about the shape and size of objects, which is necessary for many ecologically important visually guided behaviours, does pass through the sensory bottleneck. These findings show that nervous systems can be particularly economical when specific populations of cells are used for specific visually guided behaviours. This is a general-interest finding for computer vision and biomimetics, as well as sensory neuroscience.

Introduction

As with many animals, vision plays a key role in a number of behaviours performed by the fruit fly *Drosophila melanogaster*, including mate-recognition [1], place homing [2], visual course control [3], collision-avoidance [4], landing [4] and escaping a looming object (like a rolled newspaper, for example) [5]. The benefit of studying these visually guided behaviours in *Drosophila* is the range of neurogenetic techniques which give a realistic chance of understanding the neural circuits that underpin them. With that goal in mind, we focus on work by Seelig and Jayaraman [6] to map the receptive fields of a set of visually responsive neurons, the ring neurons of the ellipsoid body. These neurons are necessary and sufficient for a range of complex behaviours, such as short term spatial memory, pattern discrimination or place memory [2, 7–9], and yet are surprisingly small in number. To understand their role in these behaviours, we used modelling to bridge the gap between neurogenetic data and behaviour by evaluating ring neuron

responses during simulations of fly experiments. In this way we investigate how small populations of visual neurons in *Drosophila*, which might represent a sensory bottleneck, can still provide behaviourally relevant information.

In laboratory assays, flies show interesting spontaneous visual behaviours. For instance, flies will orient towards bar stimuli [10, 11] and in a circular arena with two diametrically placed bars will walk between them until exhaustion [12]. The attraction to vertical bars decreases as the bar is shortened and flies are strongly repulsed by small spots [13]. In addition, a number of studies have investigated the process of pattern recognition and its neural underpinnings [7, 14, 15]. Flies seem to possess a form of pattern recognition and pattern memory analogous to the better-studied pattern memory of bees [16–18]. Interestingly, both bees [19] and flies [14] fail systematically to discriminate certain pattern pairs.

These visual behaviours require the central complex, a major neuropil which comprises the ellipsoid body, the fan-shaped body, the paired noduli and the protocerebral bridge [20]. The central complex is thought to be involved primarily in spatial representation, action selection and mediation between visual input and motor output [21]. A particular class of neurons with projections in the ellipsoid body are 'ring neurons', which are known to be involved in visual behaviours (R1: place homing [2, 22, 23]; R2/R4m: pattern recognition [7, 14, 15]; R3/R4: bar fixation memory [8]). Here we investigate how the ring neurons might contribute to behaviour, by simulating the visual input as it would be processed through this small population of visually responsive cells. In particular, we can address why flies might be unable to discriminate certain pattern pairs, whether these subpopulations of neurons are optimised for pattern recognition and, if not, what visually guided behaviours these cells are suited to.

In order to do this, we leverage research which has described the receptive field properties of two classes of ring neuron in the *Drosophila* ellipsoid body [6]. The two subtypes of ring neuron investigated were the R2 and R4d ring neurons, of which only 28 and 14, respectively, were responsive to visual stimuli. The cells were found to possess receptive fields (receptive fields (RFs)) that were large, centred in the ipsilateral portion of the visual field and with forms similar to those of mammalian simple cells [24] (for details of how the receptive fields were estimated, see Materials and methods). Like simple cells, many of these neurons showed strong orientation tuning and some were sensitive to direction of motion of the stimuli. The ring neuron RFs, however, are much coarser than those of simple cells, far larger and less evenly distributed across the visual field and respond mainly to orientations near the vertical. This suggests that ring neurons might have a less general function than simple cells [25]. In mammals, the very large

population of simple cells means that small, high-contrast boundaries of any orientation are detected at all points in the visual field. Thus the encoding provided by simple cells preserves visual information and acts as a 'general purpose' perceptual network that can feed into a large number of behaviours. In contrast, the coarseness of the receptive fields of ring neurons, allied to the tight relationship between specific behaviours and specific subpopulations of ring neurons suggests instead that these cells are providing economical visual information that is likely tuned for specific behaviours [25].

To investigate such issues, we use a synthetic approach whereby investigations, in simulation, of the information provided by these populations of neurons can be related to behavioural requirements, thus 'closing the loop' between brain and behaviour. We show how the population code is well-suited to the spontaneous bar orientation behaviours shown by flies. Similarly, we verify that our population of simulated ring neurons is able to explain the success and failure of the fly to discriminate pairs of patterns. Upon deeper analysis, we demonstrate that certain shape parameters – orientation, size and position – are implicit in the ring neurons' outputs to a high accuracy, thus providing the information required for a suite of basic fly behaviours. This contrasts with the rather limited ability of ring neuron populations (and flies) to discriminate between abstract shapes, casting doubt on cognitive explanations of fly behaviour in pattern discrimination assays.

Results

Here we analyse the task-specific information provided by visually responsive ring neurons by simulating their responses during well-known behavioural experiments. To do this we use data from Seelig and Jayaraman [6] who used calcium imaging to examine the RFs of ring neurons whose cell bodies are in specific glomeruli in the lateral triangle. As the RFs of glomeruli are remarkably consistent across flies [6], we combine them to reduce measurement error and obtain sets of 'canonical' RFs, which can be thought of as visual filters. Though this averaging process will produce RFs that are more regular than those reported for individual flies, we feel this process is better than using RFs from a specific fly as, firstly, some of the irregularity in the RFs presumably derives from measurement error, and, secondly, it is unlikely that smoother edges on the RFs give an 'unfair advantage' in the tasks we examine. This process (for details, see Materials and methods) gave us a set of 28 R2 and 14 R4d filters (14 and 7 on each side, respectively). To investigate the information these cells encode, we calculate outputs for a given visual

stimulus by convolving it with the averaged ring neuron filters. This gives a population code where the outputs of the set of filters is the encoded 'representation' of the current visual stimulus. We interrogate these encodings to understand the information they contain, focusing on the relationships to specific behaviours.

Orientation towards bar stimuli

We first consider experiments in which flies are presented with bar stimuli, as flies are known to spontaneously orient towards black bars [11], aiming for the centres of narrow bars and the edges of wide bars [26]. We therefore decided to examine the responses of simulated ring neurons to bars of different widths (Figure 1A and B). The summed output of the ensembles of ring neurons shows peaks to the bars of different widths which broadly matches experimental results (Figure 1B). For instance, R2 neurons respond maximally to the inside edges of large bars, while peak activity in R4d neurons occurs at bar centres and also at roughly $\pm 90^{\circ}$. While we do not know the details of mechanisms downstream of the ring neurons and hence how their activity is transformed into action, the simulation is an existence proof that the information needed to control the observed behaviour is present in the sparse ring neuron code. We further demonstrate this point by closing the loop between sensory systems and behaviour using a simple model of a fly viewing a bar in which the fly's heading is controlled by the difference between the summed activation of left and right ring neurons (Figure 1C; see Materials and methods for details). The simulated fly approaches the bar from different distances, demonstrating centre-aiming when far from the bar and fixation of the edges when nearer and the bar's apparent size is greater (Figure 1D). Through this example, we can see how the information present in this small population of visually responsive ring neurons can control a specific behaviour. We now turn to a more complex behaviour: pattern discrimination.

Pattern discrimination in flies and ring neuron population codes

The standard paradigm involves putting a fly into a closed-loop system where it is tethered inside a drum, on the inside of which are two different visual patterns, alternating every 90°, giving four visual stimuli in total [7, 14, 15, 27] (see Figure 1E). As the fly attempts to rotate in one direction, the drum counter-rotates in closed loop, giving the illusion of the fly moving in a stable world. To elicit conditioned behaviour, if the fly faces one of the four pattern stimuli it is punished by a heat beam. Hence, if the fly can discriminate the patterns, it will learn to orient towards the non-punished pattern. Over time if the

fly is able to differentiate the patterns it will preferentially face the unpunished pattern. This procedure has been used to demonstrate that flies can differentiate stimulus pairs such as upright and inverted 'T' shapes, a small and a large square, and many others [14]. The ability to discriminate patterns in such an assay requires R2 neurons [7, 14, 28]. Specifically, synaptic plasticity afforded by *rutabaga* in these neurons is sufficient and necessary for observed pattern learning [15]. We therefore investigate the responses of ring neurons in simulations of the classic pattern discrimination paradigm.

To recreate the visual information perceived by flies in such experiments, we simulated a typical experimental flight arena with a fly tethered in the centre. We then examined the output of the ensembles of ring neurons for a fly rotating in the drum and looked at the difference in the activation code when the agent was facing the different patterns of a pair. Our logic is that if the ensemble codes were identical, it would be impossible for the patterns to be discriminated by interrogating the outputs of ring neurons alone. Similarly, the greater the difference in the ring neuron ensemble activation codes when looking at the pattern pairs, the easier they would be to discriminate (Figure 1F and G; see Materials and methods for details). Our discriminability measure is the root mean square (r.m.s.) difference between ensemble outputs when the fly faces different azimuths in the drum. In this way, we can compare the ensemble output for a simulated fly oriented at 0° (i.e. view centred on one pattern) and the ensemble output for a 'fly' at other azimuths (Figure 1). The r.m.s. difference, as compared to the view at 0°, rises as the fly rotates in the drum, peaking as it faces the space in between the patterns and dropping to a minimum when facing the centre of the next pattern (Figure 1F and G). For some pairs of patterns, there is still an appreciable r.m.s. difference between the codes when facing the centres of each pattern, thus enabling their discrimination. However, in the example of Figure 1F and G, if we displace the patterns vertically, we see a drop in the r.m.s. difference between activation codes when the fly fixates the patterns. This is despite the fact that, to the human eye, the patterns still appear very different. Interestingly, the pattern pair in Figure 1G is also harder to discriminate for flies.

In this way, we can use the difference between ensemble codes when flies face the patterns to re-examine the discriminability of pattern pairs tested with flies. One illustrative example is pattern set *(9)* from Figure 3, which contains pairs of 'triangles' (either a filled equilateral triangle, or a long and short bar arranged on top of one another), one facing up and the other down. Flies are able to discriminate these pattern pairs when they are aligned along the top and bottom, but not when aligned about the vertical centres of mass [14]. Looking at the placement and form of the R2 RFs allows us to determine where

this difference comes from (Figure 2). The excitatory regions of the RFs fall roughly across the middle of triangles that are not aligned about their vertical centres of mass and therefore the difference in width at this point will lead to differences in activation. If the triangles are offset (Figure 2) so as to be aligned about their vertical centres of mass, their width will be similar for the regions of peak R2 coverage and the difference in activation will be lower. Thus the failure to be able to discriminate features with an equivalent vertical centre of mass can be explained by the shape of the RFs interacting with the patterns directly. It is not necessary to invoke an additional system that extracts and compares the vertical centres of mass of the patterns.

Similarly, set *(2)* in Figure 3 gives examples of pattern pairs that are not discriminable by flies and also give only small differences in the outputs of R2 filters. This may seem surprising, given that these patterns appear quite different to human observers and are also very dissimilar if compared retinotopically. Thus we can see how the *Drosophila* R2 ring neuron encoding is informationally sparse. Whilst the human V1 region of human visual cortex contains neurons representing the full range of orientations all across the visual field, R2 neurons have large RFs and poor orientation resolution. Hence, a pattern pair consisting of a diagonal line facing left and a diagonal line facing right, for example, have only a small difference in R2 outputs in our simulation and are also not discriminable by flies. This could, in the light of behavioural experiments alone, be interpreted as evidence that flies do not discriminate patterns on the basis of orientation. A more parsimonious explanation, however, is that the flies are failing because the form of the RFs means that the output code is similar for these particular orientations.

To emphasise the independence of apparent similarity of patterns and the visual encoding from R2 cells, we designed shape pairs (see Materials and methods) that appear similar to humans, but are easily discriminable by the R2 population (Figure 2D and white bars in 2F), as well as shape pairs that are considered similar by the R2 population but not by human observers (or in terms of retinal overlap; Figure 2E and black bars in 2F). Despite the similarity between the pairs of patterns, the first is readily discriminable, especially from the outputs of glomeruli 1, 3, 5 and 11, while the second pair – which we easily see as having a different orientation – has very low overall differences across the glomeruli. This shows that the irregular RF shapes can lead to counterintuitive results. The small population of visually responsive R2 neurons can be though of as a sensory bottleneck. If the information that passes through this bottleneck is all that a fly has available for pattern discrimination, then we should see a close relationship between the r.m.s. difference in simulated R2 output for a pattern pair and the flies'

ability to learn to discriminate that pair. We thus examined the difference in the outputs of the R2 filters between patterns from pairs drawn from Ernst and Heisenberg [14] (Figure 3). In general, the pattern pairs for which flies show a significant learned discrimination have a greater r.m.s. difference in R2 population activity [14]. All of the pattern pairs where flies show significant learning ($n = 8$) have R2 r.m.s. differences above the overall mean (Figure 3A and B), whereas 13 out of 18 patterns that flies found more difficult to learn had below-average r.m.s. differences. (There were nine pattern pairs for which a significance level was not given that were excluded.) Across all pattern pairs, we find a significant correlation between the strength of the learning index reported for flies in [14] and the r.m.s. difference in R2 activation (Spearman's rank, $n = 30, \rho = .420, p < .05$). Of course, these differences could simply result from the apparent similarity of the patterns. Therefore, as a control comparison, we quantified the similarity of pattern pairs based on the degree to which the patterns overlap in a pixel-by-pixel manner (see Materials and methods). There was no significant correlation with the flies' learning index over the pattern pairs (Spearman's rank, $n = 32, \rho = -.068, p =$ n.s.). We additionally looked at the relationship between the two visual similarity metrics (R2 population code and pixelwise retinal overlap) and the degree to which flies show a spontaneous preference (i.e. without any conditioning) for one of the patterns within a pair (Figure 3D and E). There was no correlation for R2 population codes (Spearman's rank, $n = 29, \rho = .289, p =$ n.s.), but for retinal overlap there was a weakly significant correlation (Spearman's rank, $n = 29, \rho = -.371, p < .05$). This is consistent with research showing that R2 neurons alone are critical for learned pattern differences [14], but not spontaneous preferences which, by contrast, seem to result from activity across all subsets of ring neurons [29].

There are, however, some discrepancies where the learning performance of flies for a particular pattern pair does not match the r.m.s. difference of our R2 population code. In some cases flies are better at discriminating pairs of patterns that differ along the vertical rather than horizontal axis (set *(3)* vs set *(4)*, and the pairs in set *(12)*, marked with red Xs in Figure 3). In contrast, the r.m.s. difference in the R2 population code discriminates horizontal and vertical patterns equally. This is because while our R2 filters are being presented with static stimulus pairs to simulate a fly facing the centre of a pattern, for real flies the patterns were moving horizontally but fixed in the vertical axis making it harder for flies to resolve horizontal information [14].

Overall, we have shown that the behavioural performance of flies on a pattern discrimination task is approximated by a simple similarity metric applied to the population activity of a small number of

simulated R2 cells. However, it is curious that both flies and the population of simulated R2 cells perform badly with a number of seemingly easy pattern discriminations. Surely evolution should have selected for a simple pattern discrimination ability? A simple thought experiment is helpful in considering the purpose of the visual code provided by the R2 neurons. If we double the number of R2 neurons in our population by inserting additional RFs of the same form at random points on the visual field, then the r.m.s. difference for centre of mass-aligned triangles increases to levels similar to those for pattern pairs easily discriminated by flies (data not shown). We can therefore see how the pattern discrimination ability of an R2-like neuronal population could easily have been improved over evolutionary time without the need for any radical architectural changes, and thus we suggest that there must have been little selection pressure specifically for a specialised pattern recognition module in fruit flies.

What information is preserved in this simple neural code?

The 28 R2 and 14 R2d ring neurons condense information from 3000 ommatidia, yet are able to provide visual encodings of complex scenes. We have shown that this code provides sufficient information to discriminate some pattern pairs, but that, as performance could be improved with the addition of more ring neurons, general-purpose pattern recognition seems unlikely to be the purpose of the ring neuron system. So what information is this system tuned to extract? Examining the pattern pairs which flies and the R2 population were able to discriminate, we see that certain pattern parameters are implicitly coded for in the R2 population. Pattern sets *(6)* and *(9)* (Figure 3) suggest that, for instance, stimulus size and vertical centre of mass are parameters that can be recovered from the R2 population code after this sensory bottleneck.

Here we address in more general terms the question of what shape information is implicitly conveyed in the ring neuron population code. To do this, we generated large sets of ellipse-like 'blob' stimuli varying in size (specified by major-axis length), position (azimuth and elevation) and orientation. The blob generation procedure was stochastic and so the precise shape of each blob was random and unique (see Materials and methods). We then trained an artificial neural network (ANN) to recover this shape information from either a raw image of the shape (the control condition) or from the output of the R2/R4d populations on presentation of the blobs. Here we use ANNs as statistical engines interrogating the output of the ring neuron population code to determine if shape information is implicit to the code and has therefore passed through the sensory bottleneck. We first examined whether ANNs could be trained to

extract positional information (elevation and azimuth) of randomly generated blobs. Note that as the blobs are initially aligned about their centres of mass, elevation is equivalent to vertical centre of mass (Materials and methods). The blobs varied along four parameters: elevation ($\geq -60°$ and $\leq 60°$), azimuth ($\geq -135°$ and $\leq 0°$), orientation ($\geq 0°$ and $\leq 90°$) and major-axis length ($\geq 12.79°$ and ≤ 60). Each parameter had 22 possible values, giving a total of 234,256 ($= 22^4$) stimuli. Of these, approximately 40% ($n = 93,702$) were used for training and the remainder ($n = 140,554$) for testing. Performance on the test set (Figure 4A–D) shows that ANNs are indeed able to extract information about elevation and azimuth from any of the input types (raw, R2 or R4d). Performance was better with parameter values near the middle. At the extremes, portions of the stimuli lay outside the visual field of the simulated fly, meaning stimuli begin to disappear 'off the edge' of the visual field (Figure 4A and B), making the task harder (i.e., is it a large object projecting outside the visual field, or a smaller object at the edge?). While performance was best with raw views as inputs (Figure 4C and D), positional information could still be reliably extracted from ring neuron outputs. The R2 code performs better than the R4d and the addition of R4d RFs to the R2 code, while adding dimensionality, does not improve performance, suggesting that either an R2-like encoding is sufficient to extract positional information, or that the information in the two codes is redundant. Thus small populations of ring neurons retain positional information.

We next trained ANNs to decode information about stimulus orientation and size. The stimuli were random blobs, as before, with the same possible values for elevation, orientation and major-axis length (and thus size). This time, however, azimuthal position was fixed at $-90°$. The reason for this was that the neural network struggled to encode information about orientation when azimuth was also varied, presumably because the centres of the receptive fields – and thus the position on the visual field where they can best extract information – are clustered at around $-90°$. For this experiment there were therefore 10,648 ($= 22^3$) stimuli, of which approximately 40% ($n = 4259$) were used for training and the remainder ($n = 6389$) for testing. The ANNs were able to extract this shape information from both raw images and the ring neuron outputs (Figure 4E–H). Orientation was the parameter with the highest error score, possibly because its calculation requires a second-order statistic (the covariance of the shape). Nonetheless, both parameters could be simultaneously estimated by an ANN neural network fed with ring neuron outputs.

In summary, we have shown that information about a number of shape properties passes through the bottleneck created by the small number of ring neurons. This indicates that such information is available

downstream of the ring neurons for the guidance of behaviour.

Discussion

A general problem in neuroscience is understanding how sensory systems organise information to be at the service of behaviour. Computational approaches can be important in this endeavour, as they allow simulation of the sensory experience of a behaving animal, such that one can investigate how this information is transformed by populations of neurons into behaviour. In this way, we can relate the details of neural circuitry to theories about the requirements of behaviour. Work by Seelig and Jayaraman [6], showing the forms of visual receptive fields for ring neurons projecting to the ellipsoid body of flies, gave us the opportunity to investigate how these neurons transform information and how this information relates to specific behaviours. In particular, we have shown that despite the small size of the neural code, the outputs of the ring neurons can subserve both bar following and limited pattern recognition and also implicitly convey information about shape parameters. We now discuss the implications of our findings.

Short-term memory for object position in flies

One striking feature of the ring neuron receptive fields is that they are in general tuned to vertically oriented objects. We know that fruit flies are strongly attracted to vertical bars, a finding that has been leveraged across a range of behavioural paradigms (e.g. bar fixation: [8]). In one, single flies are placed into a virtual-reality arena, with two vertical stripes shown 180° apart, and flies typically head back and forth between the two bars. Occasionally, when a fly crosses the arena's midline, the bars disappear and a new bar is presented at 90° to the originals, to which the flies reorient. The new target then also disappears, and the flies resume their initial heading, even though the original bars are no longer visible. This indicates that directional information is stored in short-term memory and updated. Work by Neuser and colleagues [8] has shown that R4 (and R3) ring neurons are involved in this spatial orientation memory. We found that both R2 and R4d neurons were responsive to vertical bars of varying widths, mimicking flies' preference for the edges of larger bars and the centres of narrower ones [26]. We also showed that the cells provide sufficient information to guide homing towards a large vertical object and, separately, that the azimuth of bar stimuli makes it through the sensory bottleneck. Taken together, these findings demonstrate a viable role for the small R4d population in the behaviours described above.

The more general role of R4d cells within the central complex is still unknown. There is evidence that R4d neurons are able to act as a ring attractor, maintaining a stable encoding of the fly's orientation with respect to a landmark [9, 30]. Therefore, R4d neurons could be conceived variously as functioning like mammalian head-direction cells [31], playing a part in a path integration system [8] or in conditioning of visual orientation [32], perhaps serving several functions simultaneously. These possibilities are not mutually exclusive, of course, and their true function will become apparent only with a better understanding of the behaviours in which they are involved.

Do flies recognise patterns?

Drosophila can discriminate patterns differing in size, orientation and elevation and other complex shape parameters, an ability for which R2 cells are critical [7, 14, 15]. We have shown that the discriminability of a given pattern pair is predicted by the outputs of the small population of R2 cells, which have coarse receptive fields and therefore do not encode higher-order visual properties explicitly. Does this limited ability of the R2 population (and, of course, the fly) to discriminate patterns suggest that flies might be a good model for the study of a universal perceptual process of pattern recognition, or might limited pattern recognition be an artefact of a perceptual basis tuned to other tasks? Any selection pressure on flies' ability to discriminate patterns (as bees need to do, for instance) would surely have led to a larger R2 population or, possibly, visual input to the mushroom body [33, 34], and we can therefore be confident that ring neurons have not been tuned for arbitrary, general-purpose pattern recognition. Accordingly, we must suggest caution if research on flies is used with the aim of understanding the neural basis of pattern recognition or even visual cognition more generally [35]. So what behaviours are served by the information that makes it through this sensory bottleneck?

It is interesting to consider to what extent *Drosophila*'s ecological needs are served by general learning mechanisms – such as a capacity to learn arbitrary visual stimuli – and to what extent by domain-specific abilities. For example, bees have a well-attested ability to learn many varied patterns, which presumably derives from a need to learn flowers [36]; it is not apparent, however, that there has been a comparable selection pressure on *Drosophila* for such a general-purpose learning ability. Across the animal kingdom there are many cases where a task-specific heuristic can provide an elegant solution. For example, male fiddler crabs (*Uca pugilator*) treat salient objects above the horizon as predators and everything below as conspecifics [37]. Similarly, *Drosophila* have a mechanism to approach bars and to avoid small objects [13];

presumably to approach vegetation (for oviposition, etc.) and avoid predators, respectively. In order to fully understand these circuits we need to examine further how flies depend on a balance of innate visual responses versus learned visual information.

So, if the R2s are not truly 'pattern-recognition cells', the question remains: what are they for? Though we have not attempted to answer this question here, we have shown that there is *implicit* information about higher-order properties, such as stimulus position, in the RFs' code, which could drive any number of natural behaviours. For example, elsewhere we have shown that the information content of ring neuron RFs is suitable for place learning and homing [2, 38], and although this involves R1 ring neurons, not R2, it gives an indication of how small populations of coarse, wide-field cells can be used to drive behaviour. However, a set of neurons can serve diverse functions, making the story more complex: in particular, different subsets of R2 neurons have also been implicated in an olfactory decision task [39] and in sleep drive [40].

One of the advantages of studying insects is the potential for describing their neural processes with modelling. In this way, simulations can help bridge the gap between biology and behaviour [41]. **W**e have shown that the sensory bottleneck produced by small populations of cells are not a barrier to the specific information that is required for particular behaviours. However, this modelling work, and the neuroscience that invited it, do suggest caution when proposing that flies possess general visual cognition, which makes sense given the limited bandwidth of the sensory signal from the small populations. We thus hope that future experiments, grounded in both the ecological needs of the animal and the information given by neural circuits, will be able to better inform the next generation of models, and vice versa.

Materials and methods

Neurogenetic methods used for estimating ring neuron receptive fields

The goal of Seelig and Jayaraman's [6] work was to examine responses of lateral triangle microglomeruli (which house the cell bodies of the ring neurons) to visual stimuli. For this, they employed two-photon calcium imaging to examine the activity of genetically targeted subsets of microglomeruli, the R2 and R3/R4d neurons. Fluorescence was recorded for head-fixed flies held in an arena with a curved display composed of an LED array. In order to map the receptive fields, the flies were presented with a series of flashing dots at random locations on the visual display; the fine structure of the receptive fields (RFs)

was then revealed by using white-noise stimuli [42]. The accuracy of the estimated receptive fields was then verified by correlating predicted with actual responses to novel bar stimuli (and a high degree of correspondence was found).

Turning visual receptive field data into visual filters

To create the visual filters which represent RFs, we first extract the image representations of the RFs from Seelig and Jayaraman (Extended Data Figure 8 in [6]). This gives us images of 112×252 pixels for R2 neurons and 88×198 pixels for R4d. Given the visual field is taken as $120° \times 270°$, this corresponds to a resolution of $1.07°$ and $1.36°$ per pixel, respectively. As data is given for multiple flies, we averaged the RFs for the different glomeruli across flies ($2 \leq N(\text{R2}) \leq 6, 4 \leq N(\text{R4}) \leq 7$). This process is summarised in Figure 5. Each point on the is initially assigned a value ranging from –1 for maximum inhibition to 1 for maximum excitation, based on the values given by the colour scale bars in [6]. These images are then thresholded to give a kernel $g(i, j)$:

$$g(i,j) = \begin{cases} 1 & \text{for } R_{i,j} \geq T; \\ -1 & \text{for } R_{i,j} \leq -T; \\ 0 & \text{otherwise.} \end{cases}$$

where $g(i, j)$ is the (i, j)th pixel of the kernel, $R_{i,j}$ is the (i, j)th value of the processed receptive field image and T is the threshold value, here 0.25 (Figure 5A).

We take the centroid of the largest excitatory region as the 'centre' of each of the kernels. The excitatory regions are then extracted using MATLAB's `bwlabeln` function (with eight-connectivity) and the centroid, (x, y), with the `regionprops` function. The mean centroid, $(\bar{x}, \bar{y})$, across flies is then calculated and the kernels are recentred on this point:

$$\hat{g}(i,j) = \begin{cases} g(i + y - \bar{y}, j + x - \bar{x}) & \text{for } 1 \leq i + y - \bar{y} \leq m \text{ and } 1 \leq j + x - \bar{x} \leq n; \\ 0 & \text{otherwise.} \end{cases}$$

where $\hat{g}(i, j)$ is the recentred kernel (Figure 5C).

We next calculate the average kernel across flies, $\bar{g}(i,j)$, and threshold again:

$$\bar{g}(i,j) = \begin{cases} -1 & \text{for } c \leq -T; \\ 1 & \text{for } c \geq T; \\ 0 & \text{otherwise.} \end{cases}$$
$$\text{where } c = \frac{1}{|\mathbf{G}|} \sum_{\hat{g} \in \mathbf{G}} \hat{g}(i,j)$$

where $\mathbf{G}$ is the set of kernels being averaged and T is the threshold (again: 0.25). Note that instead of thresholding then averaging the raw images, R, before thresholding them again, we could have averaged the raw pixel values. The reason we did not do so was to reduce noise on the raw images; tests showed a negligible difference in performance when doing the latter.

In order to calculate the activation for a given RF to an image the RF must first be resized to the same size as the image. This is accomplished by resizing the average RF, $\bar{g}(i,j)$ (using MATLAB's `imresize` function with appropriate normalisation). Finally, the kernel is rethresholded and the excitatory and inhibitory regions are assigned different values:

$$K_{i,j} = \begin{cases} \frac{1}{N_{\text{exc}}}, & \text{for } \bar{g}(i,j) = 1; \\ -\frac{1}{N_{\text{inh}}}, & \text{for } \bar{g}(i,j) = -1; \\ 0, & \text{otherwise.} \end{cases}$$

where N_{exc} and N_{inh} indicate the number of excitatory and inhibitory pixels, respectively. This method of allocating values has the result that the activation (see below) for an all-white or -black image will be zero and was chosen because we are assuming that these filters, like edge detectors, are tuned to respond to relative differences within images and not absolute values.

The activation of an average kernel, K, to the presentation of a greyscale image, I, at rotation θ, is then:

$$A(I,K,\theta) = \sum_{i=1}^{m} \sum_{j=1}^{n} I_{i,j}(\theta) K_{i,j}, \quad \text{where } 0 \leq I_{i,j}(\theta) \leq 1 \tag{1}$$

where $I_{i,j}(\theta)$ and $K_{i,j}$ are the (i,j)th pixels of the image and kernel, respectively. This process is illustrated in Figure 5A.

Replication of behavioural experiments

The equation for describing the bar fixation mechanism shown in Figure 1C is as follows:

$$\phi_{\text{turn}} = \frac{\text{gain} \cdot \pi}{4} \left(\sum_{K \in \mathbf{G}_{\text{left}}} \max(0, A(I, K, 0°)) - \sum_{K \in \mathbf{G}_{\text{right}}} \max(0, A(I, K, 0°)) \right)$$

where I is the view of the bar from the agent's current location and $\mathbf{G}_{\text{left}}$ and $\mathbf{G}_{\text{right}}$ are the sets of left- and right-hemispheric filters. 'Gain' is a parameter to control the gain of the system, and here was set to 2.

For the pattern recognition tasks (see Figure 3), the difference in activation is calculated as follows:

$$D(I) = \sqrt{\frac{\sum_{K \in \mathbf{G}} (A(I, K, 0°) - A(I, K, 90°))^2}{|\mathbf{G}|}}$$

where $\mathbf{G}$ is the set of R2 filters, I is the current pattern pair and $A(\cdot, \cdot, \cdot)$ is the activation of the kernel to the pattern, as described in Equation 1. The retinal overlap for two binary patterns, A and B, is calculated in two steps. Firstly we measure the number of overlapping pixels between A and B; this value is referred to as Q. Next the proportion of pixels which this overlap represents for A and B is calculated and, finally, we calculate the retinal overlap as the average of these two values:

$$O(A, B) = \frac{Q}{2} \left(\frac{1}{\sum_{i=1}^{m} \sum_{j=1}^{n} A_{i,j}} + \frac{1}{\sum_{i=1}^{m} \sum_{j=1}^{n} B_{i,j}} \right)$$

where $A_{i,j}$ and $B_{i,j}$ represent the ith, jth pixel of patterns A and B, respectively.

Neural networks

The neural networks were executed using the `Netlab` toolbox for MATLAB. All networks were two-layer feedforward networks, with 10 hidden units and a linear activation function for the output units. There were 100 training cycles and optimisation was performed with the scaled conjugate gradient method.

Random blob stimuli

The stimuli used to train the networks were a series of black 'blobs' on a white background. The blobs were based on ellipses with a fixed ratio between the lengths of the major and minor axes (2 : 1), with the radii modified with complex waves:

$$r(\theta) \leq \left(\frac{\cos^2 \theta}{2} + \frac{\sin^2 \theta}{a} \right)^{-1} + W(\theta), \theta \in \{0, 2\pi\}$$

where a is the length of the major axis and $W(\theta)$ is a complex wave defined as:

$$W(\theta) = \sum_{i=1}^{n} W_i(\theta) = \sum_{i=1}^{n} A_i \sin f_i(\theta + \phi_i)$$

where A_i, f_i and ϕ_i describe the maximum amplitude, frequency and phase shift of the wave, $W_i(\theta)$, respectively. This method for generating stimuli allows for a substantial degree of random variation between the stimuli, while not producing shapes that are so irregular as to be unlearnable by a neural network.

In these experiments, A_i, f_i and ϕ_i were randomly generated and $n = 2$. A_i was a random value from 0 to 1, f_i were random integers from 1 to 30 and ϕ_i was a random value from 0 to 2π.

The blobs were first generated, according to the above equation, as images of 120×270 pixels. For the 'raw view' stimuli, these images were resized, using MATLAB's `imresize` function, to 2×14 pixels, thus giving the same number of inputs as there are R2 filters ($n = 28$).

Acknowledgements

AD, PG and AP are funded by EPSRC (grant code: EP/P006094/1). AW is funded by the Fyssen Foundation. AD and PG have also received funding from the BBSRC (grant codes: BB/F015925/1 and BB/H013644). AP has also received funding from the European Union's Seventh Framework Programme for research, technological development and demonstration under grant agreement no. 308943.

References

1. Agrawal S, Safarik S, Dickinson M (2014) The relative roles of vision and chemosensation in mate recognition of *Drosophila melanogaster*. J Exp Biol 217: 2796–2805.

2. Ofstad TA, Zuker CS, Reiser MB (2011) Visual place learning in *Drosophila melanogaster*. Nature 474: 204–207.

3. Borst A (2014) Fly visual course control: behaviour, algorithms and circuits. Nat Rev Neurosci 15: 590–599.

4. Tammero LF, Dickinson MH (2002) Collision-avoidance and landing responses are mediated by separate pathways in the fruit fly, *Drosophila melanogaster*. J Exp Biol 205: 2785–2798.

5. Card G, Dickinson MH (2008) Visually mediated motor planning in the escape response of *Drosophila*. Curr Biol 18: 1300–1307.

6. Seelig JD, Jayaraman V (2013) Feature detection and orientation tuning in the *Drosophila* central complex. Nature 503: 262–266.

7. Liu G, Seiler H, Wen A, Zars T, Ito K, et al. (2006) Distinct memory traces for two visual features in the *Drosophila* brain. Nature 439: 551–556.

8. Neuser K, Triphan T, Mronz M, Poeck B, Strauss R (2008) Analysis of a spatial orientation memory in *Drosophila*. Nature 453: 1244–1248.

9. Seelig JD, Jayaraman V (2015) Neural dynamics for landmark orientation and angular path integration. Nature 521: 186–191.

10. Reichardt W, Wenking H (1969) Optical detection and fixation of objects by fixed flying flies. Naturwissenschaften 56: 424–424.

11. Götz KG (1987) Course-control, metabolism and wing interference during ultralong tethered flight in *Drosophila melanogaster*. J Exp Biol 128: 35–46.

12. Strauss R, Heisenberg M (1993) A higher control center of locomotor behavior in the *Drosophila* brain. J Neurosci 13: 1852–861.

13. Maimon G, Straw AD, Dickinson MH (2008) A simple vision-based algorithm for decision making in flying *Drosophila*. Curr Biol 18: 464–470.

14. Ernst R, Heisenberg M (1999) The memory template in *Drosophila* pattern vision at the flight simulator. Vision Res 39: 3920–3933.

15. Pan Y, Zhou Y, Guo C, Gong H, Gong Z, et al. (2009) Differential roles of the fan-shaped body and the ellipsoid body in *Drosophila* visual pattern memory. Learn Mem 16: 289–295.

16. von Frisch K (1914) Der Farbensinn und Formensinn der Biene. Zool Jahrb 35: 1–188.

17. Giurfa M, Menzel R (1997) Insect visual perception: complex abilities of simple nervous systems. Curr Opin Neurobiol 7: 505–513.

18. Horridge GA (2009) What does the honeybee see and how do we know?: A critique of scientific reason. Canberra: ANU E Press.

19. Srinivasan MV, Zhang SW, Witney K (1994) Visual discrimination of pattern orientation by honeybees: performance and implications for 'cortical' processing. Phil Trans R Soc B 343: 199–210.

20. Young JM, Armstrong JD (2010) Structure of the adult central complex in *Drosophila*: organization of distinct neuronal subsets. J Comp Neurol 518: 1500–1524.

21. Pfeiffer K, Homberg U (2014) Organization and functional roles of the central complex in the insect brain. Annu Rev Entomol 59: 165–184.

22. Sitaraman D, Zars M, LaFerriere H, Chen YC, Sable-Smith A, et al. (2008) Serotonin is necessary for place memory in *Drosophila*. Proc Natl Acad Sci USA 105: 5579–5584.

23. Sitaraman D, Zars T (2010) Lack of prediction for high-temperature exposures enhances *Drosophila* place learning. J Exp Biol 213: 4018–4022.

24. Hubel DH, Wiesel TN (1962) Receptive fields, binocular interaction and functional architecture in the cat's visual cortex. J Physiol (Lond) 160: 106–154.

25. Wystrach A, Dewar ADM, Graham P (2014) Insect vision: emergence of pattern recognition from coarse encoding. Curr Biol 24: R78–R80.

26. Osorio D, Srinivasan MV, Pinter RB (1990) What causes edge fixation in walking flies? J Exp Biol 149: 281–292.

27. Dill M, Wolf R, Heisenberg M (1993) Visual pattern recognition in *Drosophila* involves retinotopic matching. Nature 365: 751–753.

28. Wang Z, Pan Y, Li W, Jiang H, Chatzimanolis L, et al. (2008) Visual pattern memory requires *foraging* function in the central complex of *Drosophila*. Learn Mem 15: 133–142.

29. Solanki N, Wolf R, Heisenberg M (2015) Central complex and mushroom bodies mediate novelty choice behavior in *Drosophila*. J Neurogenet 29: 1–16.

30. Cope AJ, Sabo C, Vasilaki E, Barron AB, Marshall JAR, et al. (2017) A computational model of the integration of landmarks and motion in the insect central complex. PLOS ONE 12: e0172325.

31. Tomchik SM, Davis RL (2008) Behavioural neuroscience: out of sight, but not out of mind. Nature 453: 1192–1194.

32. Guo C, Du Y, Yuan D, Li M, Gong H, et al. (2015) A conditioned visual orientation requires the ellipsoid body in *Drosophila*. Learn Mem 22: 56–63.

33. Ehmer B, Gronenberg W (2002) Segregation of visual input to the mushroom bodies in the honeybee (apis mellifera). J Comp Neurol 451: 362–373.

34. Wolf R, Wittig T, Liu L, Wustmann G, Eyding D, et al. (1998) *Drosophila* mushroom bodies are dispensable for visual, tactile, and motor learning. Learn Mem 5: 166–178.

35. Menzel R, Giurfa M (2001) Cognitive architecture of a mini-brain: the honeybee. Trends Cogn Sci 5: 62–71.

36. Gould JL (1985) How bees remember flower shapes. Science 227: 1492–1494.

37. Layne J, Land M, Zeil J (1997) Fiddler crabs use the visual horizon to distinguish predators from conspecifics: a review of the evidence. J Mar Biol Assoc UK 77: 43–54.

38. Dewar ADM, Wystrach A, Graham P, Philippides A (2015) Navigation-specific neural coding in the visual system of *Drosophila*. Biosystems 136: 120–127.

39. Azanchi R, Kaun KR, Heberlein U (2013) Competing dopamine neurons drive oviposition choice for ethanol in *Drosophila*. Proc Natl Acad Sci USA 110: 21153–21158.

40. Liu S, Liu Q, Tabuchi M, Wu MN (2016) Sleep drive is encoded by neural plastic changes in a dedicated circuit. Cell 165: 1347–1360.

41. Webb B (2009) Animals versus animats: Or why not model the real iguana? Adapt Behav 17: 269–286.

42. Weber F, Machens CK, Borst A (2010) Spatiotemporal response properties of optic-flow processing neurons. Neuron 67: 629–642.

43. Götz KG (1980) Visual guidance in *Drosophila*. In: Siddiqi O, Babu P, Hall LM, Hall JC, editors, Development and Neurobiology of *Drosophila*, Springer US, volume 16 of *Basic Life Sciences*. pp. 391–407. doi:10.1007/978-1-4684-7968-3_28.

44. Bülthoff H, Götz KG, Herre M (1982) Recurrent inversion of visual orientation in the walking fly, *Drosophila melanogaster*. J Comp Physiol 148: 471–481.

Figure Legends

Figure 1. Simulation of two behavioural experiments with *Drosophila* to examine the outputs of the R2 and R4d RFs. A: A diagram showing Buridan's paradigm [43, 44]. If a fly is placed in an arena between two large vertical bars, it will walk back and forth until exhaustion. B: The mean output of R2 (blue) and R4d (green) filters to bars of different widths from two points in the arena (blue +) across headings. C: The summed outputs of R2 and R4d filters can be used to drive orientation towards a bar stimulus with a simple proportional-integral-derivative (PID) controller. D: A vector field of orientations for a simulated fly driven by the simple PID controller. Note that this is not intended as a descriptive model of how bar attraction in flies operates, but as an illustration of the information latent in the outputs of the ring neurons, hence why many of the 'flies' in the vector plot would miss the bar. E: The fly is held tethered in a drum. As the fly attempts to rotate about its yaw-axis, the drum rotates in the opposite direction, thus allowing the fly to select the portion of the pattern in view. By monitoring the fly's heading, one can surmise whether there is a spontaneous preference for one of the patterns. Whether the fly can learn to head towards one pattern is tested by adding a laser that punishes the fly for facing one of the patterns. Shown inside the drum are the visual RFs for one pair of left- and right-hemispheric glomeruli. F and G: The r.m.s. difference in output for R2 RFs as the pattern is rotated. The reference activities are the RF outputs when the simulated flies are at 0°. Patterns with a greater difference in activity at 0° *vs* 90° (indicated by dotted lines) should be more discriminable by flies. For two pairs of patterns we show that there is a much smaller difference in output when the triangles are aligned about the vertical centre of mass (F) than not (G). This mirrors real flies' performance on this task [14].

Figure 2. R2 cells do not encode detailed shape information. A–C: The discriminability of pattern pairs can vary greatly independently of the apparent difference between visual stimuli. A: A pattern pair made up of a triangle and its inverse with both triangles aligned to their lowest points. B: The same triangles, but this time aligned by their centres of mass, make another pattern pair. C: The difference in activation between 0° and 90° for all R2 RF filters for the triangles from A (white bars) and B (black bars). The mean activation difference is greater for the triangles in A than in B. The red square marks the output of the ring neuron RF shown in A and B. D–F: We can also generate shapes that appear similar yet produce a large mean difference in RF activation (D) or appear different and produce similar RF activations (E). The stimuli here are 'blobs' of the form described in Materials and methods. An optimisation was performed in MATLAB (`fminsearch` function) to minimise the ratio of blob difference to difference in activation (D) or its inverse (E). Pairs of stimuli are shown in grey and green whereas in the simulation both are black. F: The corresponding activations of the different R2 RFs to the blobs in D and E. Two similar patterns give a mean difference in activity of 11.0% and two very different patterns give a mean difference in activity of 5.10%. The dotted line indicates the mean activation for the blob in D and the dashed line for the blob in E.

Figure 3. Outputs of simulated R2 cells and degree of retinal overlap for published pattern pairs. Difference in R2 RF output partly predicts whether patterns are discriminable by flies, but not whether there is a spontaneous preference. By contrast, retinal overlap predicts whether there is a spontaneous preference, but not whether the patterns will be discriminable. The patterns tested here are drawn from [14] and are grouped according to the figures in which they appear in that work; the corresponding figure numbers are shown in parentheses. All patterns for which the significance of 'learning preference' ($\overline{\text{DCP}}$) was given are included. A: Grey bars indicate that the $\overline{\text{DCP}}$ for the pattern was significant ($p < .05$). A higher score indicates a greater r.m.s. difference in R2 activity and thus that the pattern was more discriminable by the simulation. Performance on more 'horizontal' patterns (e.g. *(3)* and the final three patterns in *(12)*) was poor in the behavioural experiments, but better in simulation. This is perhaps due to the horizontal motion of the patterns in training, as noted in [14]. B and C: Scatter plots of R2 difference (the 'RF Model') and retinal overlap (the 'Retinotopic Model') *vs* spontaneous preference ($\overline{\text{SCP}}$) shown in [14]. A significant correlation was found for the Retinotopic Model ($n = 29; \rho = -0.370509; p < .05$) but not the RF Model (Spearman's rank, $n = 29, \rho = .289, p =$ n.s.). D and E: Scatter plots of R2 difference (the 'RF Model') and retinal overlap *vs* learning index ($\overline{\text{DCP}}$). A significant correlation was found for the RF Model (Spearman's rank, $n = 32, \rho = .502, p < .005$) but not the Retinotopic Model ($n = 32, \rho = -.00960, p =$ n.s.). As two data points on the far right in panel D could be outliers, we reran the analysis excluding these points and found that the correlation was still significant, albeit less so ($n = 30, \rho = .420, p < .05$).

Figure 4. How much shape information is preserved in the R2 population code? Neural networks were trained to estimate various properties of randomly generated 'blob' stimuli ($N = 10,000$) from raw views ($N = 36$ pixels; blue), R2 neurons ($N = 28$; red), R4d neurons ($N = 14$; green) or R2 and R4 neurons ($N = 42$; magenta). Panels A–D show results for networks trained with elevation and azimuth and panels E–H for size and elevation. For each visual input a network was trained 100 times and average performance with blobs that were not part of the training set was taken. A and B: Plots of elevation and azimuth of the test visual stimuli *vs* the mean network output ($N = 100$). The dashed line indicates ideal performance (i.e. $y = x$) and the thickness of the lines at each point shows standard error. The possible values of elevation and azimuth were constrained by the size of the fruit fly visual field (approx. $120° \times 270°$). Within this range there were 22 possible values. C and D: Average network performance (mean square error) for networks trained to recover elevation (C) or azimuth (D) and for each type of visual input (colour code as above). Standard error is shown, but is very small. E and F: Network performance in recovering stimulus orientation and size. Orientation was constrained between $0°$ and $90°$, to avoid the problem of aliasing, and varied with 22 levels. G and H: Average network performance (mean square error) for networks trained to recover orientation (C) or size (D) and for each type of visual input (colour code as previously). Standard error is shown, but is very small.

Figure 5. The algorithm for obtaining average RFs. A: The raw image (left; fly glomerulus 1) is thresholded so as to give excitatory and inhibitory regions of uniform intensity (right). The 'centre' is then calculated as the centroid of the largest excitatory region (+). B: Aligning two RFs. The new centre is taken as the average of the centre of both RFs and the RFs are then shifted so that the centres are aligned. C: Averaging the RFs for this glomerulus over all flies ($N = 7$), following alignment. Note that this the left-hemispheric version; the right-hemispheric version is its mirror. D: Averaged R2 and R4d filters.

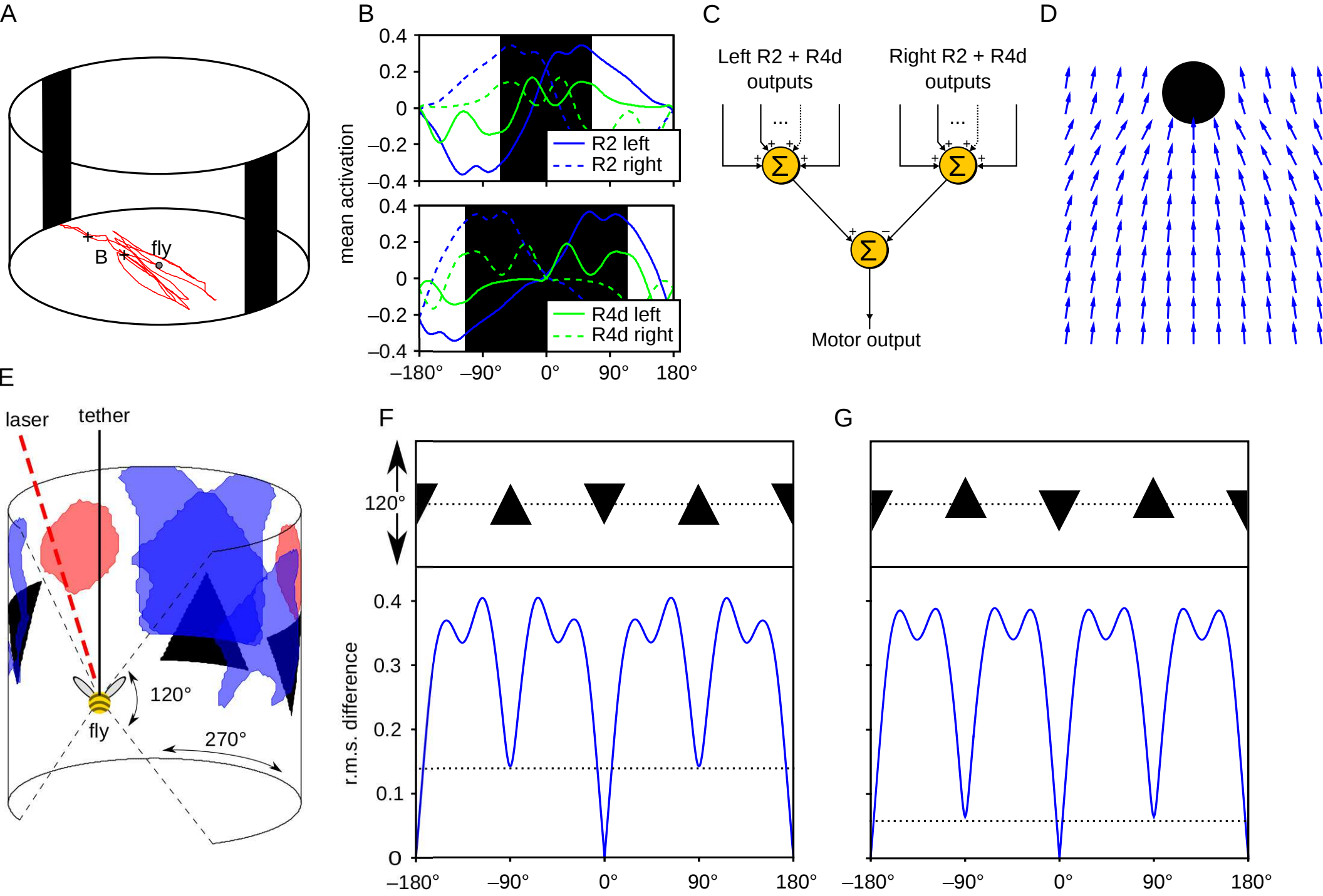

Figure 2

Click here to download Figure Fig2.eps

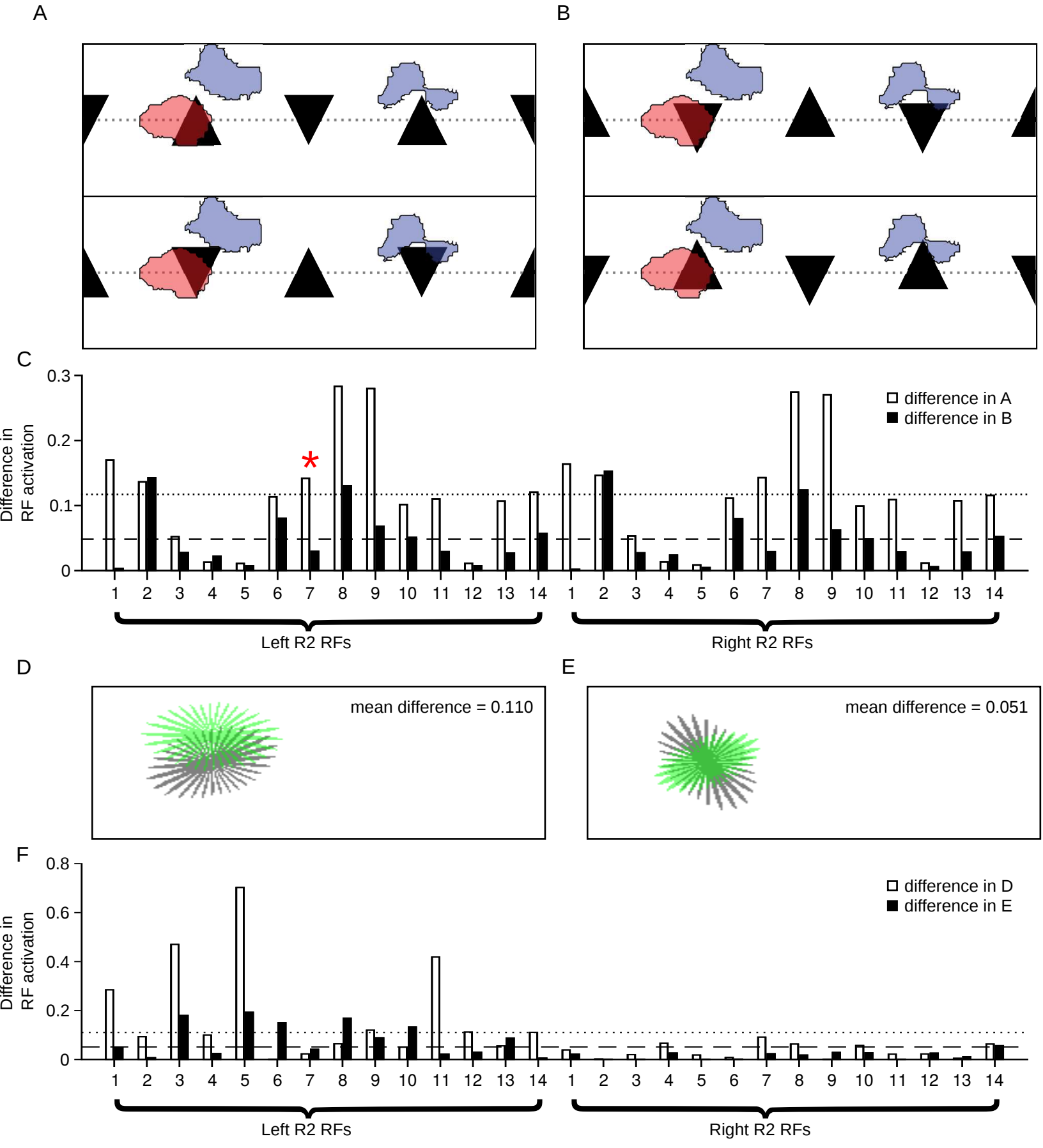

Figure 3

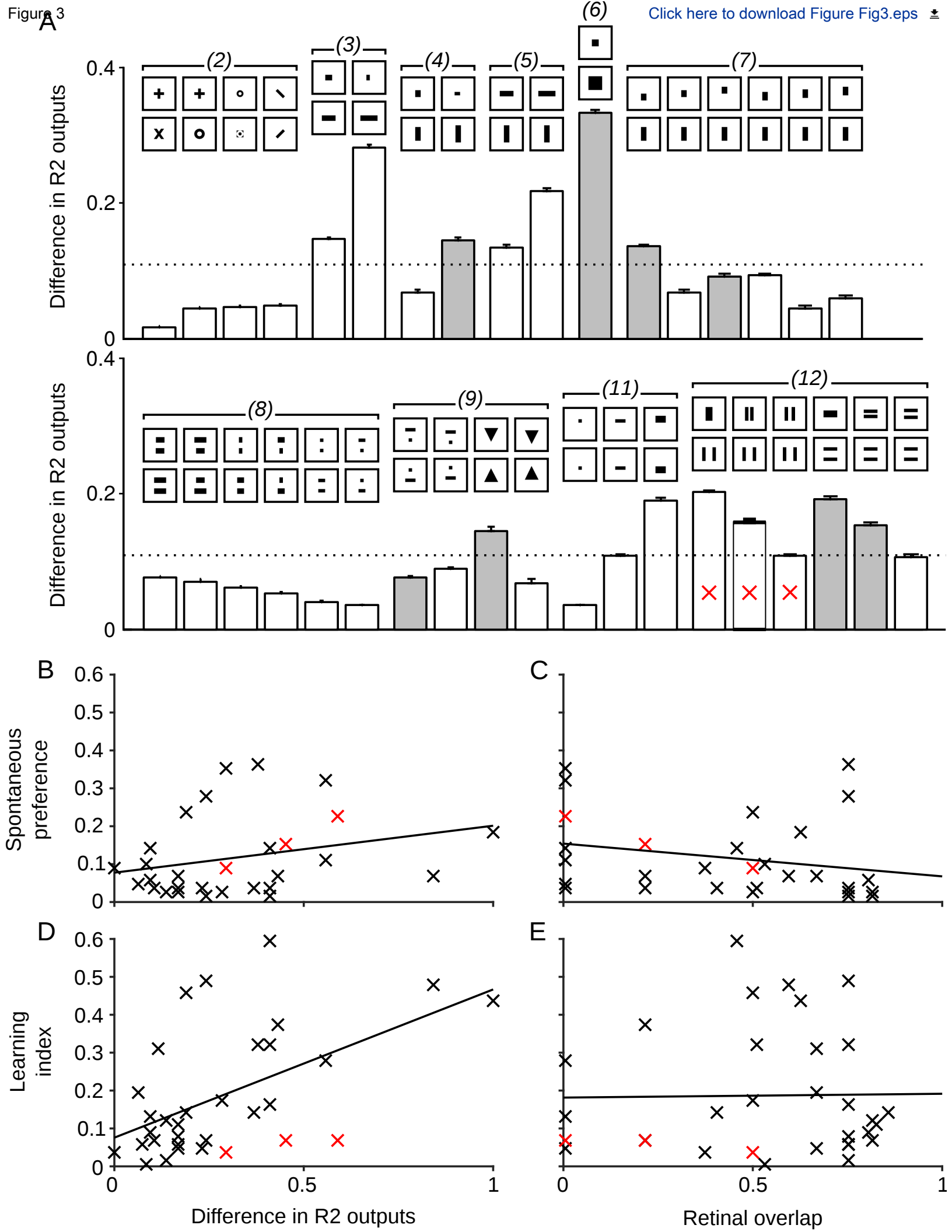

Figure 4

Click here to download Figure Fig4.eps

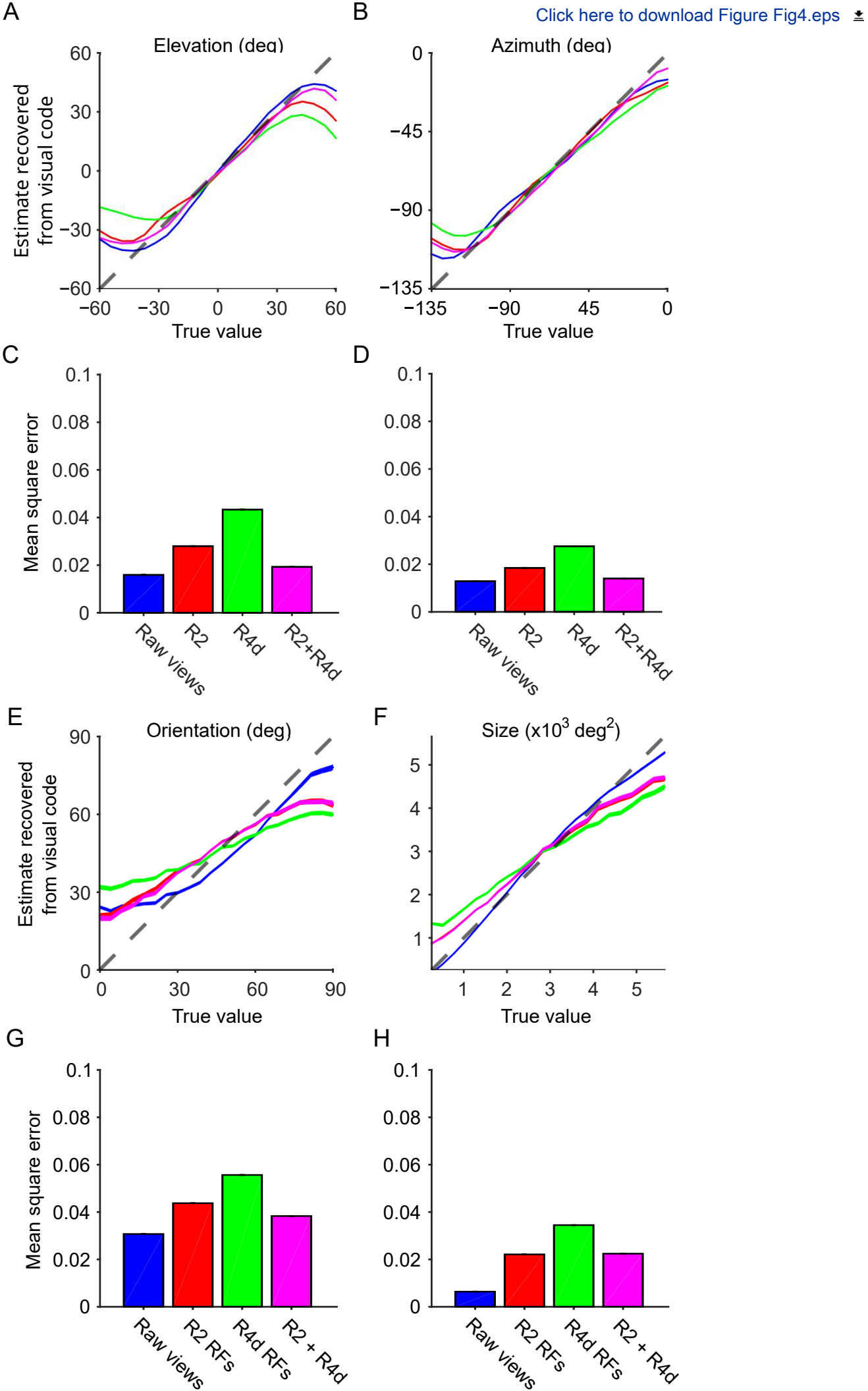

Figure 5

Click here to download Figure Fig5.eps